

Self-Assembly of Islands on Spherical Substrates by Surface Instability

Xiangbiao Liao,[†] Junfeng Xiao,[‡] Yong Ni,[§] Chaorong Li,[⊥] and Xi Chen^{*,†,||}

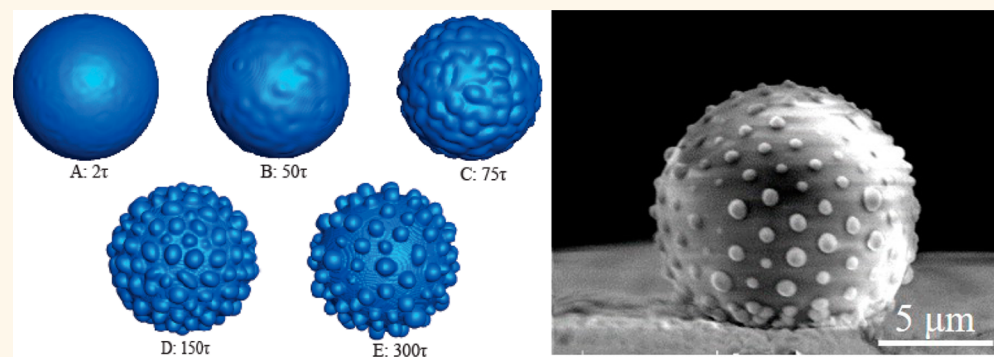
[†]Department of Earth and Environmental Engineering and [‡]Department of Mechanical Engineering, Columbia University, New York, New York 10027, United States

[§]CAS Key Laboratory of Mechanical Behavior and Design of Materials, University of Science and Technology of China, Hefei 230026, China

[⊥]Center for Optoelectronics Materials and Devices, Department of Physics, Zhejiang Sci-Tech University, Hangzhou 310018, China

^{||}School of Chemical Engineering, Northwest University, Xi'an 710069, China

S Supporting Information



ABSTRACT: Through strain-induced morphological instability, protruding patterns of roughly commensurate nanostructures are self-assembled on the surface of spherical core/shell systems. A three-dimensional (3D) phase field model is established for a closed substrate. We investigate both numerically and analytically the kinetics of the morphological evolution, from grooves to separated islands, which are sensitive to substrate curvature, misfit strain, and modulus ratio between the core and shell. The faster growth rate of surface undulation is associated with the core/shell system of a harder substrate, larger radius, or misfit strain. On the basis of a Ag core/SiO₂ shell system, the self-assemblies of SiO₂ nanoislands were explored experimentally. The numerical and experimental studies herein could guide the fabrication of ordered quantum structures *via* surface instability on closed and curved substrates.

KEYWORDS: closed and curved substrates, surface instability, ordered quantum structures, misfit strain

Surface instability of thin films not only plays a critical role in the evolution of surface morphologies observed in natural and biological systems^{1–3} but also underpins a promising micro/nanofabrication technique for mechanical self-assembly of surface patterns.^{4–6} Many previous studies of surface instability were based on spontaneous wrinkles in stiff film/compliant substrate systems. These have demonstrated the feasibility and tunability of two-dimensional (2D) patterns of thin films on planar substrates, including stripes,^{7–9} herringbones, and zigzag labyrinths, by varying the anisotropy of membrane force.^{10–13} Studies on curved and closed substrates were inspired by the observation of the triangular/Fibonacci patterns of spherules on the Ag core/SiO₂ shell microstructures upon cooling.^{14–16} Intensive theoretical models and experiments were then carried out to investigate the spontaneous organization of 3D wrinkling morphologies such as buckyball-

like, labyrinth-like, and ridged patterns in spheroidal systems^{1,11,17,18} with controllable geometrical/material parameters.

Nevertheless, an intriguing mystery remains unresolved. In the pioneering study of the instability of the curved surface of Ag core/SiO₂ shell microstructures, the mechanism of wrinkling/buckling failed to explain the protruding features of spherules.^{14,16} The buckling theory can deduce only dent-like morphologies, but not the more interesting protruding ones. Since the pioneering work has been widely cited, its unreasonable explanation misled a large amount of scholars working in this field. Due to the big impact from the misinterpretation, a sound clarification of the mechanism behind spherule patterns on

Received: October 20, 2016

Accepted: March 8, 2017

Published: March 8, 2017

spherical substrates is urgent. In fact, in those Ag core/SiO₂ shell microsystems the ratio of surface energy to strain energy is comparable with the typical roughness wavelength,¹¹ and at the high annealing temperature of 1270 K the surface diffusion of SiO₂ becomes noticeable.^{14,19} However, the classic buckling analysis¹¹ can incorporate neither surface energy nor mass diffusion. Here we propose a mechanism where the formation of such protruding morphologies may be controlled by the competition between strain energy and surface energy as well as surface diffusion. The elucidation of the mechanism of diffusion-controlled surface instability may not only help to explain the spontaneous islands on spherical core/shell microstructures but also enrich the pathways of mechanical self-assembly.

The morphological instability based on diffusion in strained thin films was elucidated by Asaro Tiller, Grinfeld, and Srolovitz (referred to as ATG instability).^{20–22} The growth of thin films on lattice-mismatched substrates, such as InGaAs/GaAs and Si_{1-x}Ge_x/Si,^{23,24} usually follows the ATG instability mode. This can lead to the evolution of various surface morphologies, such as crack-like grooves, ripples, and islands. Unlike those on planar substrates, anticorrelated islands,^{19,25} and periodic shells,^{4,26} which were observed to evolve on cylindrical nanowire surfaces, this implies the controllability of morphologies by size and curvature.

Inspired by these experimental results, extensive studies have theoretically explored the stability and kinetics of the surface morphology. The critical parameters and initial modes of instability in various planar film/substrate^{27,28} or cylindrical^{19,29,30} systems were deduced through linear perturbation analysis. The competition between two stress–relaxation mechanisms during the epitaxial growth of thin films—misfit dislocation and undulation of free surface—was also investigated.^{28,31} To explore the nonlinear surface evolution, significant research efforts have been devoted to various numerical methods. On the basis of the Galerkin finite element methods, Yang *et al.* predicted the formation of ordered quantum structures in strained epitaxial films^{32,33} and core/shell nanowires.³⁴ Free from singularities, the phase field model by the Ginzburg–Landau approach is a promising numerical technique. The simultaneous growth and coarsening of quantum islands was obtained in two- and three-dimensional (3D) phase field simulations.^{35,36} Furthermore, the method was used to quantitatively explore the controllability of self-assembled patterns on planar and curved substrates by tuning geometrical size and elastic and misfit-strain anisotropies.^{4,36–38}

Despite these advances, the study of ATG instability of closed and curved thin films/substrate systems is rare. Among the limited literature, the microstructural stability and evolution of one particle in contact with its melt subjected to mass rearrangement and a growing spherical precipitate–matrix interface has been analytically and numerically explored.^{39–41} Although Colin deduced the growth rate of fluctuation in the case of two stressed spherical shells,⁴² the elastic heterogeneity was not considered. The mechanism of stressed-driven instability *via* surface diffusion in spherical core/shell systems remains unclear. Indeed, surface instability modes of closed core/shell systems (such as spherical) could enrich the family of surface diffusion-driven assembly of spontaneous patterns on curved microstructures and complement those induced by buckling. In this study, the linear perturbation analysis considering elastic heterogeneity is analytically performed and linked to the surface instability at the very initial stage. In addition, using 3D phase

field modeling, we numerically explore the nonlinear evolution of surface instability on the spherical core/shell microstructures in the presence of misfit strain. The geometrical/material properties and misfit strain affecting the kinetics of morphological evolution are discussed, which qualitatively echoes those predicted by linear analysis. Finally, we experimentally explore the controlled self-assemblies on spherical Ag core/SiO₂ shell microstructures to verify the pattern features of islands.

RESULTS AND DISCUSSION

A model of a spherical core/shell composite (Figure 1) is established using spherical coordinates to investigate the surface

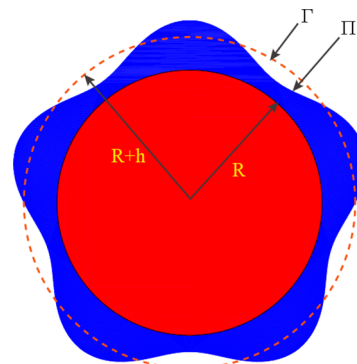


Figure 1. Schematic of a spherical core/shell structure: the radius of the core is denoted by R , and the shell has a thickness h . Γ and Π respectively denote the initial morphology and that after surface instability.

instability of a thin film enclosing a closed and curved substrate under stress. The core and shell with isotropic elasticity have different shear moduli, μ_c and μ_s ($\beta = \mu_c/\mu_s$), while the Poisson ratio ν is taken to be the same for simplicity. An isotropic intrinsic strain $\epsilon^* = H(r - R)\text{diag}(\epsilon^*, \epsilon^*, \epsilon^*)$ is introduced in the core, and the interface between core and shell is assumed to be coherent without involving misfit dislocations. Basically, the intrinsic strain can mimic the misfit of thermal expansion or the lattice mismatch in epitaxial crystalline growth during the annealing process.⁴²

Linear Stability Analysis. To study the combined effect of substrate radius R , modulus ratio β , and eigenstrain ϵ^* on the kinetics of morphological evolution, we extend Colin's work⁴² for our case of spherical core/shell microstructure, where β does not equal 1 (refer to the Supporting Information). The growth rate (see eq S3) can be reduced to that in Colin's work⁴² with the special case of $\beta = 1$. The critical radius, below which the fluctuation may not develop, is determined from the expression $(1 + h/R)^5 = 21(1 - \nu)\alpha R/[2(7 + 5\nu)R^*]$. It is apparent that the critical radius is sensitive to the modulus ratio and eigenstrain, matching those in previous works.^{39,41–43} The typical parameters, $\epsilon^* = 0.02$, $\gamma = 1.5 \text{ J m}^{-2}$, $\mu_s = 30 \text{ GPa}$, and $\nu = 0.3$,¹¹ are taken; they correspond to the Ag core/SiO₂ shell system in the parallel experiment below, and their variations with temperature are neglected.^{35,36}

On the basis of eq S3, relating the growth rate to fluctuation amplitude, the positive growth rate leads to development of a fluctuating morphology, whereas a stable surface results from the negative value. We plot the dimensionless growth rate ω as a function of degree l for increasing normalized sizes R/h in Figure 2a. It is observed that with an increasing value of R/h , not only the number of the mode degree l for a positive growth rate but

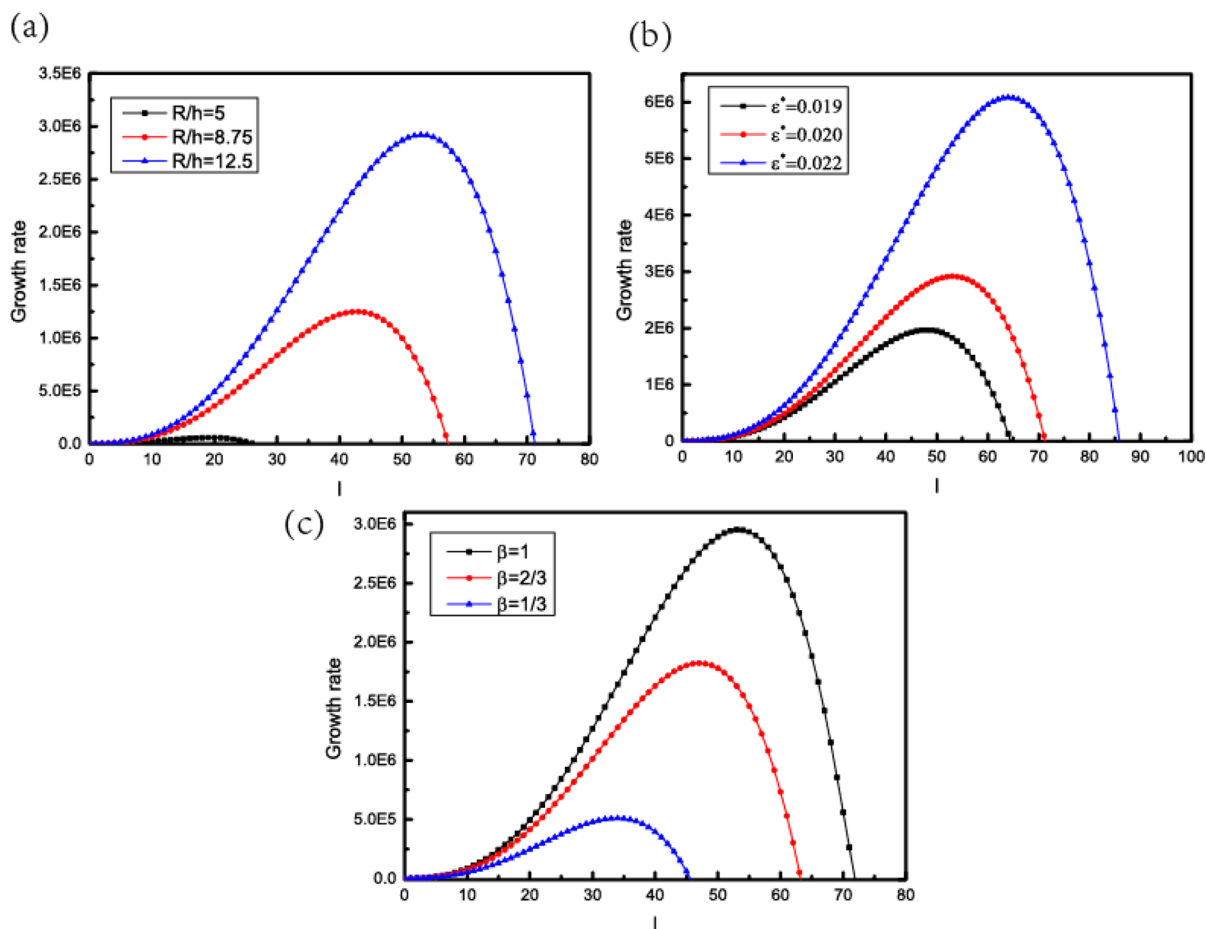


Figure 2. Dimensionless growth rate, characterizing the evolution of fluctuation amplitude in the system with $\epsilon^* = 0.02$, $\gamma = 1.5 \text{ J m}^{-2}$, $\mu_s = 30 \text{ GPa}$, and $\nu = 0.3$, plotted as a function of various fluctuation mode degree l characterizing the evolving morphology at various values of (a) normalized size R/h , (b) intrinsic strain ϵ^* , and (c) modulus ratio β .

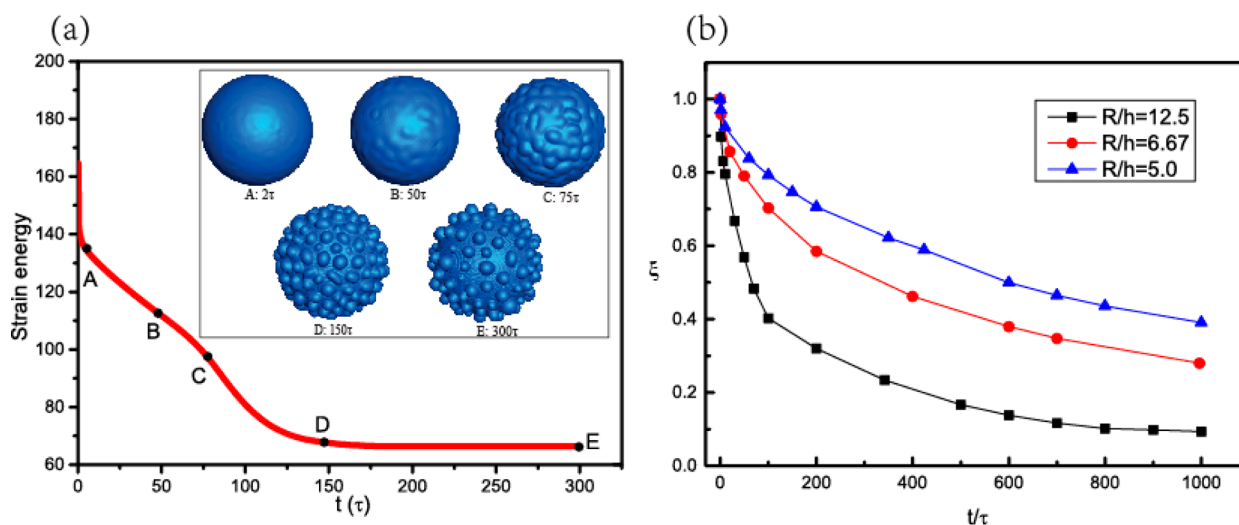


Figure 3. (a) Evolution of strain energy of the spherical core/shell particle ($R = 50l$, $h = 4l$, $\beta = 1/3$) as a function of dimensionless time. The inset shows the surface morphologies at different evolution times. (b) Coverage parameter ξ as a function of simulation time for three cases: $R/h = 12.5$; $R/h = 6.67$; $R/h = 5.0$ (intrinsic strain $\epsilon^* = 0.02$, modulus ratio $\beta = 1/3$, constant volume of the shell).

also the value of the growth rate increases. Thus, the amplitude of a perturbed surface grows faster in the system with a larger R/h value. Furthermore, the most possible instability mode l_f is defined to correspond to the fastest growth rate among all perturbation modes, and it refers to the typical wavenumber of

the rough surface after instability. As shown in Figure 2a, the value of l_f decreases as the normalized size R/h is reduced, implying a denser morphology in a larger structure just at the initial stage of surface undulation. Similar trends were also revealed in Colin's work with $\beta = 1$.

In addition, the effects of eigenstrain and modulus ratio on the growth rate are shown in Figure 2b and c, respectively. It can be noticed that the surface roughness of a misfit-strained system develops slower than the one with larger misfit strain, and the growth rate of the fluctuated morphology decreases as the modulus ratio of core to shell decreases. Retracting and comparing the values of l_f in Figure 2b and c, we can expect a denser protruding pattern in the structure with either larger modulus ratio or intrinsic strain. Therefore, the linear stability analysis preliminarily underlines the controllability of self-assembled morphologies on a spherical substrate.

Nonlinear Dynamics Simulation. Since the above-mentioned analysis predicts only the surface evolution at the very initial stage, we adopt a 3D phase field approach^{35–37} to study the nonlinear surface instability (see the [Experimental Details](#) section for details). The development of the surface undulation in a representative spherical core/shell structure with misfit strain is shown in the inset of Figure 3a. As the simulation time proceeds, the morphological pattern evolves from initial fluctuation (described as eq S10) to a flat surface ($t = 2\tau$), several grooves ($t = 50\tau$), ripples ($t = 75\tau$), and islands ($t = 150\tau$). Even though the coarsening of islands continues after $t = 150\tau$, the topology of the pattern after $t = 300\tau$ changes little and thus suggests the system is fairly close to the equilibrium state due to the extremely slow growth rate thereafter. It is noted that within the context of the mesh roughness and initial random fluctuations the close-to-equilibrium pattern of islands should be regarded as quasi-periodic.

The strain energy of the system is plotted as a function of dimensionless time in Figure 3a. It clearly shows that the development of surface roughness is associated with elastic energy relaxation, followed by a plateau where the islands coarsen. Specifically, the first stage ($t = 0 - 2\tau$) of stress relaxation corresponds to the smoothening of initially random undulation. Subsequently, as shown in Figure 3a, the relaxation of strain energy has two fast stages: the formation of grooves until exposure of the substrate ($A \rightarrow B \rightarrow C$) and the breaking of ripples into a set of islands ($C \rightarrow D$). The reduction of strain energy implies that the formation of islands is thermodynamically driven. Finally, there is a slower process ($D \rightarrow E$) corresponding to island refinement due to the achievement of stress relaxation. Moreover, the small variation of strain energy ($D \rightarrow E$) verifies the kinetically unfavorable process of the further coarsening and refinement of islands, since both the slow growth rate and numerical imperfections make it difficult for the evolution of an ideally periodic pattern with commensurate islands within a limited simulation time. The quasi-equilibrium pattern of islands on a spherical substrate is very likely to be the result of stress relaxation due to surface instability, not due to deformation as mechanical buckling.^{5,13}

To quantitatively explore the kinetics of morphological evolution, the coverage parameter ξ characterizing the extent of surface evolution is defined as the percentage of mass left inside the otherwise smooth, nonevolving surface (dashed circle in Figure 1), e.g., $\xi = 1$ at the beginning of surface instability. The extent of evolution ξ as a function of time t is plotted in Figure 3b for increasing values of substrate curvature. It is seen that the growth rate, denoted by the slope of the curves, decreases exponentially with simulation time. This can be compared with the morphological evolution in Figure 3a, which illustrates the fast evolution occurring at the initial times and close to equilibrium after $t = 400\tau$. Furthermore, the faster evolution is evidently associated with a larger substrate radius, showing the

curvature-dependent kinetics of undulation growth and a unique feature of the closed and curved substrate. The results in Figure 2a bear a resemblance to the trends here, although they are valid only at the very initial stage of surface instability. Therefore, the self-assembly of small spherules on a spherical substrate is feasible through tuning the evolution time and substrate curvature, implying an alternative route to future fabrication of ordered structures on spherical substrates.

Furthermore, the effects of normalized size R/h , eigenstrain ε^* , and modulus ratio β were explored. Unless otherwise noted, the results below are for the shell having a thickness of $h = 4l$ and shear modulus $\mu_s = 30$ GPa. Besides the coverage parameter ξ , the dimensionless average height (normalized to l) of the island peaks relative to the initial radius of the shell, $R + h$, is another quantitative parameter to describe the extent of undulation. Due to the mass conservation in a given system, the increase of average height roughly corresponds to the decrease in the number of islands. A morphological map at $t = 100\tau$ is constructed with respect to the substrate radius and intrinsic strain in Figure 4a, which shows the transition from stable surface

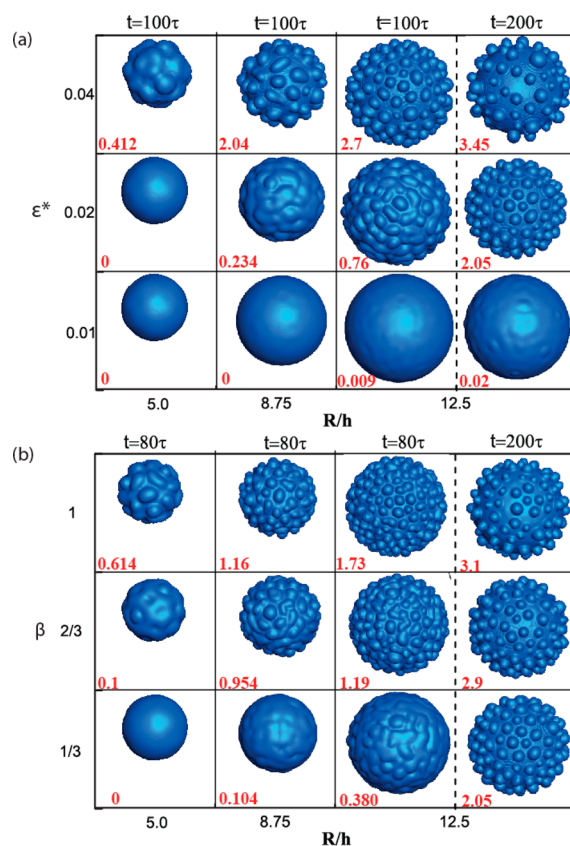


Figure 4. Diagrams for surface morphology at given times (a) $t = 80\tau$ and (b) $t = 100\tau$. The morphologies of the structure ($R/h = 12.5$) at $t = 200\tau$ are shown on the right side of (a) and (b); the dimensionless average heights of undulation are highlighted in red.

to the pattern of separated islands. For a given value of R/h , the surface undulation grows faster with the increase of ε^* , and when ε^* is fixed, the grooves change to islands as the substrate curvature is reduced. In addition, the distribution of islands on the substrate is denser than that on the substrate with a smaller radius. Moreover, the average heights not only illustrate the undisturbed morphology when both R/h and ε^* are small, implying the existence of a critical curvature corresponding to a

stable surface, but also validate the amplitude of undulations growing faster in larger particles, as revealed by the linear analysis.

In the second morphological map in Figure 4b, the spontaneous patterns at $t = 80\tau$ are selected to further study the competition of geometrical parameter R/h and modulus ratio β between core and shell. From the cases with a certain value of R/h , the transition from grooves to islands occurs earlier in the systems with a harder substrate. On the basis of the diagram, it is evident that the denser distribution of islands is favored when β and R/h become larger. Meanwhile, the effect of larger modulus ratio resulting in faster morphological evolution is consolidated by the average height of the islands shown in Figure 4b. Comparing with $t = 80\tau$ and $t = 100\tau$ in Figure 4a and b, respectively, the morphologies at $t = 200\tau$ show a decreasing number of islands, with an increase in the dimensionless average height. The maps in Figure 4 provide a promising and controllable way for self-assembling ordered structures on spherical substrates by controlling the evolution time, geometrical/material properties, and misfit strain.

In the 3D simulation above-mentioned, the difference of the diffusivity in the surface, interface, and bulk is neglected in the phase field model for simplicity, and the surface diffusion could be much faster than the others, whose role will be explored in the future. The intrinsic strain and elastic properties adopted in the current study may be regarded as effective averaged parameters. Through uncovering some of the essential factors affecting the dynamics of diffusional surface evolution, the model could be refined to incorporate more complicated geometries, temperature-dependent and anisotropic elasticity, and eigenstrain parameters, which possibly offers ways to design various surface topologies on the closed/curved substrate. Parallel experimental realizations are explored below to enrich our purposes.

Experiments. As discussed above, uniform islands are able to be self-assembled on the closed and curved substrate (e.g., spherical substrate) through the mechanism of diffusional surface instability, the kinetics of which is highly dependent on substrate curvature, mismatch strain, and modulus ratio between the substrate and shell. In this section, the morphologies with protruding features are experimentally studied with emphasis on the spherical Ag core/SiO₂ shell microstructures, which may promise manipulation of 3D patterns on closed and curved substrates.

Ag core/SiO₂ shell samples were synthesized by thermal evaporation of a SiO and Ag₂O mixture into sapphire substrates, which was heated to 1270 K. Before cooling, we kept the system at 1535 K for different durations in order to investigate the effect of annealing time. The profiles of the Ag core/SiO₂ shell microstructures, annealed for 1, 5, and 10 min, are respectively shown in Figure 5a, b, and c. The chemical compositions of Ag, Si, and O at the red dashed region in Figure 5c were characterized

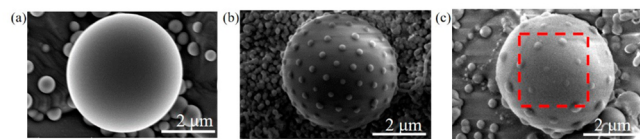


Figure 5. Three representative surface patterns of the Ag core/SiO₂ shell microstructures with an approximate radius of 2.5 μm: (a) smooth surface; (b) uniform islands; (c) relatively sparse and bigger islands. The annealing times are respectively (a) 1 min, (b) 5 min, and (c) 10 min.

by the energy-dispersive X-ray spectrometer (Figure S1, Supporting Information). These three samples have approximately the same diameter of 5 μm and with more time allowed the morphological transition from smooth surface to uniform islands and finally to relatively sparse and bigger islands. Although the misfit strain in the film can drive surface undulation, the mass diffusion of SiO₂ in Figure 5a is insignificant, and its surface remains smooth due to the short annealing time. However, given the longer annealing time in Figure 5b, the uniform island-like spherules are likely the result of adequate diffusion. When the core/shell microstructure is further annealed, surface diffusion is responsible for island coarsening, which is exemplified by Figure 5c. The experimental transition from Figure 5a to c is consistent with the numerically simulated morphologies illustrated in the inset of Figure 3a (A → D → E), although it is very difficult to experimentally capture the fast transition from state A to C in Figure 3a. This transition is similar to the experimental observations in the diffusion-based growth of the Si core/Ge shell nanowire, during which the extended time for annealing makes smaller islands disappear while larger islands continue to coarsen, resulting in the morphology with low island density.¹⁹ Additionally, it is evident that the average distance between islands in Figure 5b (roughly 0.5 μm) is smaller than that in Figure 5c (roughly 1.0 μm), which further confirms the coarsening of islands as the annealing time increases. Therefore, the formation of protruding features in Figure 5b and c is likely to be diffusion-controlled.

Defects may induce nonuniformity in the core/shell structure. The profile (Figure S2, Supporting Information) shows nonuniform islands near the interface between the microstructure and sapphire substrate, while nearly uniform islands can be seen in the region far from the interface. The local nonuniformity may be induced by geometrical constraints. We also find that a large cooling rate (500 K/min) could lead to broken structures, shown in Figure 6d, which is possibly due to the fast, large thermal mismatch stress occurring in the SiO₂ shell.

In addition, the size of formed Ag core/SiO₂ shells in the vapor can be controlled by the base pressure, and the ratio of AgO₂/SiO₂ powders determines the thickness of the SiO₂ layer.⁴⁴ Thus,

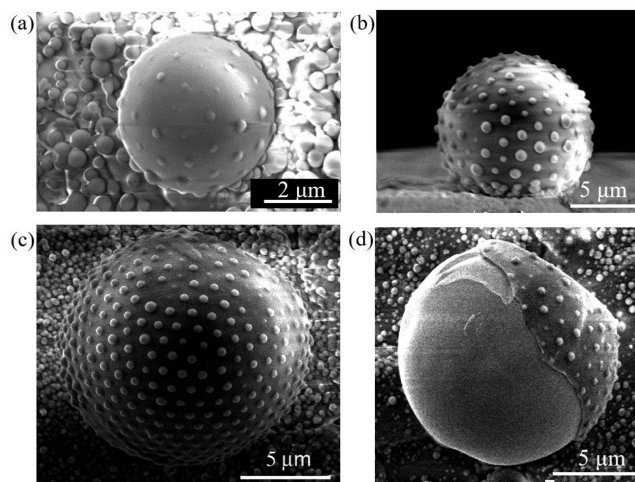


Figure 6. SEM micrographs of the Ag core/SiO₂ shell microstructures annealed for 10 min, with approximate radii of (a) 2.5 μm, (b) 4.0 μm, and (c) 7.5 μm. A broken sample with smooth Ag core partially covered by a SiO₂ shell is shown in (d) under a cooling rate of 500 K/min.

we kept the mass ratio of Ag₂O/SiO powders as 5:1, and the Ag core/SiO₂ shell microstructures with a radius of 1–10 μm were obtained by varying the base pressure within the range of 3 × 10⁴ to 4 × 10⁴ Pa. Then we annealed the system for 5 min before cooling it. The thickness of the SiO₂ layer can be measured as 150 nm from some broken structures similar to that in Figure 6d, and the thickness is approximately constant among the microstructures with various sizes due to the unchanged composition of the Ag₂O/SiO precursor. As shown in Figure 6, spontaneous SiO₂ spherules are observed on spherical Ag substrates (where β ≈ 1/3, ε* ≈ 0.02), with approximate radii of 2.5 μm for (a), 4.0 μm for (b), and 7.5 μm for (c). The observation of a denser array of islands on larger microstructures is in qualitative agreement with both numerical results in Figure 4 and analytical predictions in Figure 2a. Interestingly, the smooth surface of the exposed Ag core, shown in Figure 5d, verifies no deformation in the substrate. The evidence excludes the mechanism of mechanical buckling, which would result in the dent-like and ridged patterns for the same microstructures.^{1,11} These agreements effectively strengthen the diffusion-controlled mechanism behind the formation of islands on spherical substrates.

CONCLUDING REMARKS

In summary, the nonlinear phase field simulations and linear stability analysis are performed to explore the spontaneous patterns induced by diffusional surface instability on spherical core/shell systems. At a given evolution time, the transition of morphologies, from flat surface, to grooves and ripples, and eventually the assembly of islands with roughly uniform size, could be controlled since the growth rate of undulation is highly dependent on the substrate curvature, modulus ratio, and intrinsic strain. With the increased eigenstrain, radius, and stiffness of the substrate, the self-organization occurs faster. In parallel experiments, the surface patterns of SiO₂ islands are also successfully formed on a Ag substrate. Thus, the surface instability *via* diffusion may dominate the self-assembly of islands on spherical particles observed in a pioneering study,¹⁴ whose mechanism remains obscure until the present study. The studies here appear to be a theoretical attempt to explore the self-assembled patterns on a closed and curved substrate by the ATG instability mode, which may inspire various applications of micro/nanofabrication. It is important to note that some kinds of defects are possibly induced by stress in the interface of the core/shell, including misfit dislocation and delamination, which contributes a lot to the final morphologies.^{24,45} The investigation of the effects of such defects, along with the refinement of material and system parameters, will be the subject of future research.

On a curvature-dependent and closed substrate, the stress generated in the film, upon mismatched strain between the film and substrate, is possibly anisotropic and nonuniform. Also, the surface instability may be constrained in local regions where the boundary effect can further interact with the substrate curvature effect. These enable more varieties of morphological patterns *via* surface diffusion, which underpins self-assembly fabrication of true 3D microstructures and devices. Thus, the study of self-assembling morphological patterns *via* surface diffusion on a closed and curved substrate significantly expands applications in electronics, biomedical engineering, and optical technologies.^{43,46,47}

EXPERIMENTAL DETAILS

The detailed experimental setup and parameters can be found in the previous work.^{14,16} After evaporating the mixture of Ag₂O/SiO₂ powders in a Al₂O₃ crucible chamber, it was filled with a gas mixture of 90% Ar + 10% H₂ to a pressure of 3 × 10⁴ to 4 × 10⁴ Pa. The size of the formed Ag core/SiO₂ shells in the vapor can be controlled by the base pressure, and the ratio of the Ag₂O/SiO₂ powders determines the thickness of the SiO₂ layer. Ag core/SiO₂ shell microstructures were collected on a sapphire substrate placed 1 cm over the powder mixture's surface. At the beginning, the power mixture was heated to ~1535 K and the substrate was kept at ~1270 K. Liquid droplets were formed on the way flying to the substrate and then evolved to a Ag core/SiO₂ shell structure due to the poor miscibility between Ag and SiO₂. The Ag core/SiO₂ shell microstructures with a radius of 1–10 μm were observed on the substrate. For a controlled study of surface roughness, three groups of SiO₂ shell/Ag core microstructures were annealed at the same temperature but for different durations. Then, we cooled the system at a fast rate of ~350 K/min such that the evolved morphologies at the high annealing temperature could be kept. The morphologies of the core/shell structures were imaged through *ex situ* observation using a scanning electron microscope (SEM; FEI, SERION). The elemental compositions of the core and shell were verified from the energy-dispersive X-ray spectrometer.

ASSOCIATED CONTENT

Supporting Information

The Supporting Information is available free of charge on the ACS Publications website at DOI: 10.1021/acsnano.6b07108.

Supporting experimental results and calculation details for the linear stability analysis and nonlinear dynamics simulation (PDF)

AUTHOR INFORMATION

Corresponding Author

*E-mail: xichen@columbia.edu.

ORCID

Xiangbiao Liao: 0000-0001-8214-454X

Notes

The authors declare no competing financial interest.

ACKNOWLEDGMENTS

X.C. acknowledges the support from the National Natural Science Foundation of China (11172231 and 11372241), ARPA-E (DE-AR0000396), and AFOSR (FA9550-12-1-0159); X.L. and J.X. acknowledge the China Scholarship Council for financial support. Y.N. acknowledges the Strategic Priority Research Program of the Chinese Academy of Sciences (Grant No. XDB22040502).

REFERENCES

- (1) Yin, J.; Chen, X.; Sheinman, I. Anisotropic Buckling Patterns in Spheroidal Film/Substrate Systems and Their Implications in Some Natural and Biological Systems. *J. Mech. Phys. Solids* **2009**, *57*, 1470–1484.
- (2) Bargel, H.; Neinhuis, C. Tomato (*Lycopersicon Esculentum* Mill.) Fruit Growth and Ripening as Related to the Biomechanical Properties of Fruit Skin and Isolated Cuticle. *J. Exp. Bot.* **2005**, *56*, 1049–1060.
- (3) Dervaux, J.; Ben Amar, M. Morphogenesis of Growing Soft Tissues. *Phys. Rev. Lett.* **2008**, *101*, 101.
- (4) Day, R. W.; Mankin, M. N.; Lieber, C. M. Plateau-Rayleigh Crystal Growth of Nanowire Heterostructures: Strain-Modified Surface Chemistry and Morphological Control in 1, 2 and 3 Dimensions. *Nano Lett.* **2016**, *16*, 2830.

- (5) Chen, X.; Yin, J. Buckling Patterns of Thin Films on Curved Compliant Substrates with Applications to Morphogenesis and Three-Dimensional Micro-Fabrication. *Soft Matter* **2010**, *6*, 5667–5680.
- (6) Xia, Y.; Whitesides, G. M. Soft Lithography. *Annu. Rev. Mater. Sci.* **1998**, *28*, 153–184.
- (7) Huang, Z. Y.; Hong, W.; Suo, Z. Nonlinear Analyses of Wrinkles in a Film Bonded to a Compliant Substrate. *J. Mech. Phys. Solids* **2005**, *53*, 2101–2118.
- (8) Audoly, B.; Boudaoud, A. Buckling of a Stiff Film Bound to a Compliant Substrate—Part I. *J. Mech. Phys. Solids* **2008**, *56*, 2401–2421.
- (9) Song, J.; Jiang, H.; Liu, Z. J.; Khang, D. Y.; Huang, Y.; Rogers, J. A.; Lu, C.; Koh, C. G. Buckling of a Stiff Thin Film on a Compliant Substrate in Large Deformation. *Int. J. Solids Struct.* **2008**, *45*, 3107–3121.
- (10) Jin, H.-C.; Abelson, J. R.; Erhardt, M. K.; Nuzzo, R. G. Soft Lithographic Fabrication of an Image Sensor Array on a Curved Substrate. *J. Vac. Sci. Technol., B: Microelectron. Process. Phenom.* **2004**, *22*, 2548–2551.
- (11) Cao, G.; Chen, X.; Li, C.; Ji, A.; Cao, Z. Self-Assembled Triangular and Labyrinth Buckling Patterns of Thin Films on Spherical Substrates. *Phys. Rev. Lett.* **2008**, *100*, in press DOI: 10.1103/PhysRevLett.100.036102.
- (12) Moon, M.-W.; Lee, S. H.; Sun, J.-Y.; Oh, K. H.; Vaziri, A.; Hutchinson, J. W. Controlled Formation of Nanoscale Wrinkling Patterns on Polymers Using Focused Ion Beam. *Scr. Mater.* **2007**, *57*, 747–750.
- (13) Li, B.; Cao, Y.-P.; Feng, X.-Q.; Gao, H. Mechanics of Morphological Instabilities and Surface Wrinkling in Soft Materials: A Review. *Soft Matter* **2012**, *8*, 5728–5745.
- (14) Li, C.; Zhang, X.; Cao, Z. Triangular and Fibonacci Number Patterns Driven by Stress on Core/Shell Microstructures. *Science* **2005**, *309*, 909–911.
- (15) Li, C. R.; Dong, W. J.; Gao, L.; Cao, Z. X. Stressed Triangular Lattices on Microsized Spherical Surfaces and Their Defect Management. *Appl. Phys. Lett.* **2008**, *93*, 034108.
- (16) Li, C.-R.; Ji, A.-L.; Gao, L.; Cao, Z.-X. Stressed Triangular Tessellations and Fibonacci Parastichous Spirals on Ag Core/SiO₂ Shell Microstructures. *Adv. Mater.* **2009**, *21*, 4652–4657.
- (17) Li, B.; Jia, F.; Cao, Y.-P.; Feng, X.-Q.; Gao, H. Surface Wrinkling Patterns on a Core-Shell Soft Sphere. *Phys. Rev. Lett.* **2011**, *106*, in press DOI: 10.1103/PhysRevLett.106.234301.
- (18) Yin, J.; Cao, Z.; Li, C.; Sheinman, I.; Chen, X. Stress-Driven Buckling Patterns in Spheroidal Core/Shell Structures. *Proc. Natl. Acad. Sci. U. S. A.* **2008**, *105*, 19132–5.
- (19) Kwon, S.; Chen, Z. C. Y.; Kim, J.-H.; Xiang, J. Misfit-Guided Self-Organization of Anticorrelated Ge Quantum Dot Arrays on Si Nanowires. *Nano Lett.* **2012**, *12*, 4757–4762.
- (20) Asaro, R. J.; Tiller, W. A. Interface Morphology Development During Stress Corrosion Cracking: Part I. Via Surface Diffusion. *Metall. Trans. A* **1972**, *3*, 1789–1796.
- (21) Grinfeld, M. *Equilibrium Shape and Instabilities of Deformable Elastic Crystals*; Lecture given at Heirot-Watt University, Edinburgh, 1989.
- (22) Srolovitz, D. J. On the Stability of Surfaces of Stressed Solids. *Acta Metall.* **1989**, *37*, 621–625.
- (23) Ozkan, C. S.; Nix, W. D.; Gao, H. Strain Relaxation and Defect Formation in Heteroepitaxial Si_{1-x}Ge_x Films Via Surface Roughening Induced by Controlled Annealing Experiments. *Appl. Phys. Lett.* **1997**, *70*, 2247–2249.
- (24) Eaglesham, D. J.; Cerullo, M. Dislocation-Free Stranski-Krastanow Growth of Ge on Si(100). *Phys. Rev. Lett.* **1990**, *64*, 1943–1946.
- (25) Pan, L.; Lew, K.-K.; Redwing, J. M.; Dickey, E. C. Stranski-Krastanow Growth of Germanium on Silicon Nanowires. *Nano Lett.* **2005**, *5*, 1081–1085.
- (26) Day, R. W.; Mankin, M. N.; Gao, R.; No, Y.-S.; Kim, S.-K.; Bell, D. C.; Park, H.-G.; Lieber, C. M. Plateau-Rayleigh Crystal Growth of Periodic Shells on One-Dimensional Substrates. *Nat. Nanotechnol.* **2015**, *10*, 345–352.
- (27) Spencer, B. J.; Voorhees, P. W.; Davis, S. H. Morphological Instability in Epitaxially Strained Dislocation-Free Solid Films: Linear Stability Theory. *J. Appl. Phys.* **1993**, *73*, 4955.
- (28) Gao, H.; Nix, W. D. Surface Roughening of Heteroepitaxial Thin Films. *Annu. Rev. Mater. Sci.* **1999**, *29*, 173–209.
- (29) Wang, H.; Upmanyu, M.; Ciobanu, C. V. Morphology of Epitaxial Core-Shell Nanowires. *Nano Lett.* **2008**, *8*, 4305–4311.
- (30) Duan, H. L.; Weissmüller, J.; Wang, Y. Instabilities of Core-Shell Heterostructured Cylinders Due to Diffusions and Epitaxy: Spheroidization and Blossom of Nanowires. *J. Mech. Phys. Solids* **2008**, *56*, 1831–1851.
- (31) Tersoff, J.; LeGoues, F. K. Competing Relaxation Mechanisms in Strained Layers. *Phys. Rev. Lett.* **1994**, *72*, 3570–3573.
- (32) Zhang, Y. W.; Bower, A. F. Numerical Simulations of Island Formation in a Coherent Strained Epitaxial Thin Film System. *J. Mech. Phys. Solids* **1999**, *47*, 2273–2297.
- (33) Long, F.; Gill, S. P. A.; Cocks, A. C. F. Effect of Surface-Energy Anisotropy on the Kinetics of Quantum Dot Formation. *Phys. Rev. B: Condens. Matter Mater. Phys.* **2001**, *64*, 121307.
- (34) Guo, J. Y.; Zhang, Y. W.; Shenoy, V. B. Morphological Evolution and Ordered Quantum Structure Formation in Heteroepitaxial Core-Shell Nanowires. *ACS Nano* **2010**, *4*, 4455–62.
- (35) Wang, Y. U.; Jin, Y. M.; Khachaturyan, A. G. Phase Field Microelasticity Modeling of Surface Instability of Heteroepitaxial Thin Films. *Acta Mater.* **2004**, *52*, 81–92.
- (36) Ni, Y.; He, L. H.; Soh, A. K. Three-Dimensional Phase Field Simulation for Surface Roughening of Heteroepitaxial Films with Elastic Anisotropy. *J. Cryst. Growth* **2005**, *284*, 281–292.
- (37) Ni, Y.; He, L. H. Spontaneous Formation of Vertically Anticorrelated Epitaxial Islands on Ultrathin Substrates. *Appl. Phys. Lett.* **2010**, *97*, 261911.
- (38) Ni, Y.; He, L. H.; Liao, X. B. Stress Anisotropy Controlled Morphological Evolution in Core-Shell Nanowires. *Extreme Mechanics Letters* **2016**, *8*, 160.
- (39) Mullins, W. W.; Sekerka, R. F. Morphological Stability of a Particle Growing by Diffusion or Heat Flow. *J. Appl. Phys.* **1963**, *34*, 323–329.
- (40) Li, X.; Lowengrub, J.; Nie, Q.; Cristini, V.; Leo, P. Microstructure Evolution in Three-Dimensional Inhomogeneous Elastic Media. *Metall. Mater. Trans. A* **2003**, *34*, 1421–1431.
- (41) Leo, P. H.; Iwan, J.; Alexander, D.; Sekerka, R. F. Elastic Fields About a Perturbed Spherical Inclusion. *Acta Metall.* **1985**, *33*, 985–989.
- (42) Colin, J. Morphological Instability of Two Stressed Spherical Shells. *Int. J. Solids Struct.* **2007**, *44*, 3218–3230.
- (43) Hu, J.; Ouyang, M.; Yang, P.; Lieber, C. M. Controlled Growth and Electrical Properties of Heterojunctions of Carbon Nanotubes and Silicon Nanowires. *Nature* **1999**, *399*, 48–51.
- (44) Gao, L.; Ji, A.; Lu, N.; Li, C.; Cao, Z. Fast Vapor Phase Growth of SiO₂ Nanowires Via Surface-Flow on Ag Core/SiO₂ Shell Structure. *AIP Adv.* **2012**, *2*, 012187.
- (45) Hutchinson, J. W. Delamination of Compressed Films on Curved Substrates. *J. Mech. Phys. Solids* **2001**, *49*, 1847–1864.
- (46) Stangl, J.; Holý, V.; Bauer, G. Structural Properties of Self-Organized Semiconductor Nanostructures. *Rev. Mod. Phys.* **2004**, *76*, 725–783.
- (47) Li, Y.; Qian, F.; Xiang, J.; Lieber, C. M. Nanowire Electronic and Optoelectronic Devices. *Mater. Today* **2006**, *9*, 18–27.